

2024

Increasing the Service Life of Marine Transport Using Heat-Resistant Polymer Nanocomposites

Sapronov, O

<https://pearl.plymouth.ac.uk/handle/10026.1/22324>

10.3390/ma17071503

Materials

MDPI AG

All content in PEARL is protected by copyright law. Author manuscripts are made available in accordance with publisher policies. Please cite only the published version using the details provided on the item record or document. In the absence of an open licence (e.g. Creative Commons), permissions for further reuse of content should be sought from the publisher or author.

Increasing the service life of marine transport using heat-resistant polymer nano-composites

Oleksandr Sapronov^{1, *}, Andriy Buketov¹, Boksun Kim², Pavlo Vorobiov¹, Lyudmila Sapronova¹

¹ Department of Transport Technologies and Mechanical Engineering, Kherson State Maritime Academy, Ushakova Avenue, 20, 73003 Kherson, Ukraine; oo.sapronov@gmail.com (O.S.); buketov@tntu.edu.ua (A.B.); Vorobyov020291@gmail.com (P.V.); 2023sapronova2023@gmail.com (L.S.)

² School of Engineering, Computing and Mathematics, University of Plymouth, Drake Circus, Plymouth PL4 8AA, UK; boksun.kim@plymouth.ac.uk (B.K.)

Abstract: This paper presents the technological aspects of increasing the thermal stability of polymers. Epoxy binder used to form polymer materials. Polyethylene polyamine is used to crosslink the epoxy binder. To ensure the thermal stability of polymer, nano-dispersed condensed carbon with a dispersion of 10-16 nm is used. Research of nano-composites under the influence of elevated temperatures is carried out using the "Thermoscan-2" derivatograph. Complex studies of thermophysical properties are carried out, according to the results of which the optimal content of nano-filler (0.050 pts.wt). At the same time, such a polymers is characterized by the following properties: temperature of the beginning of mass loss – $T_0 = 624.9$ K; final temperature of mass loss – $T_f = 718.7$ K; relative mass loss – $\varepsilon_m = 60.3\%$. Researched of the activation energy of thermal destruction is performed to determine the resistance to the destruction of chemical bonds. It is proved that the maximum value of activation energy (170.1 kJ/mol) is characterized by nano-composites with a content of nano-dispersed condensed carbon 0.050 pts.wt., which indicates the thermal stability of the polymer.

Keywords: nano-dispersed condensed carbon; nano-composite; activation thermal destruction; infrared spectroscopy

1. Introduction

Thanks to their improved mechanical, physical, and chemical properties, reactive plastics are used as adhesive materials or multi-functional products in many industries [1-9]. In terms of corrosion resistance, reactive plastic polymers are enormously superior to metals and their alloys [10-13], so they can be used as protective coatings. When operating parts of transport equipment such as hull parts of the ship. Under the influence of high temperatures and pressure, ensure efficiency the indicators of polymers.

The research background of the study is that unfilled reaction-plastic polymer materials do not provide high thermal stability [14-18] and are characterized by one of the disadvantages that limits their use – a low temperature at thermal destruction [19-22]. In addition, in the works [14-17, 32, 33] presents the technology of forming composite materials with nano particles, which includes complex technological modes, in particular: functionalization in a solvent, solvent removal, ultrasonic dispersion, grafting of surface-active groups, vacuuming. That is, the forming technology becomes more complicated and, accordingly, the forming time and the cost of the polymer material increase.

Therefore, the main task of scientific research is to ensure the thermal stability of polymers by choosing a thermally stable additive. As well as simplifying the technology of polymer material formation.

Carbon nanofillers, such as nanotubes, fullerenes, nanocarbon black, graphene, etc., are used to improve strength characteristics and prevent thermal destruction or increase the temperature at which the combustion process occurs [16, 18, 23-25]. The authors [26-28] investigated the course of the process of thermal destruction of polymers. These provisions are consistent with the results of the research given in the work by authors [18-25]. Therefore, the use of chemical methods of influencing the processes of thermo-oxidative destruction, will allow changing the structure of such materials by introducing active nano-sized particles into the polymer matrix. Nanodispersed condensed carbon is the starting product in the detonation synthesis of nanodiamonds. As well as fullerene black or fullerene soot, formed during the synthesis of fullerenes. However, if the characteristics of fullerene soot and fullerene black are inferior to fullerenes, then nanodispersed condensed carbon is similar in characteristics to nanodiamonds. Therefore, the main reason for the use of nanodispersed condensed carbon is its characteristics, in particular: the specific surface area of nanodispersed condensed carbon is 280-460 m²/g, while the specific surface area of nanodiamond is 270-330 m²/g; the pore volume of nanodispersed condensed carbon is 0.6-0.9 cm³/g, while that of nanodiamond is 0.6-1.1 cm³/g, which is quite close in absolute value.

In terms of morphology, microstructure, elemental composition, and reactivity, nano-dispersed condensed carbon and nanodiamonds are close to each other. The main difference is that the crystal structure of nano-dispersed condensed carbon is hexagonal, and that of nanodiamond is cubic. Thus, the highly deformed state of the crystal lattice nano-dispersed condensed carbon is thermally stable. This creates interest in the development of thermostable epoxy composites. This, in turn, will ensure a change in the mechanism and speed of chemical destruction reactions, and, therefore, a change in the thermo-oxidative destruction by inhibiting these reactions.

In addition, it should be noted that the cost of nanodispersed condensed carbon is 40% lower than nanodiamond, which affects the cost performance of the final product, and therefore the scale of production polymer materials.

2. Materials and Methods

2.1. Materials

Epoxy oligomer ED-20 was used as a binder (ISO 18280:2010), which was hardened with polyethylene polyamine (Technical Regulations TU 6-05-241-202-78, Technobudresurs, Kyiv, Ukraine).

Nano-dispersed condensed carbon (NCC) (YongFeng Chemicals Company, Hefei, China) obtained by detonation synthesis. The size of nanoparticles of amount $d \approx 10-16$ nm. The starting temperature of NCC oxidation is 583-623 K.

2.2. Material-Forming Technology

To improve the degree of nanoparticle wetting (the main cause of polymer delamination), and, therefore, the interphase interaction of the polymer-nanoparticle system, epoxy composites are formed:

- preliminary dosing of oligomer, heating to a temperature of 353 ± 2 K and holding during for a time of 20 ± 0.1 min;
- dosage of nano-dispersed condensed carbon;
- introduction of nano-dispersed condensed carbon into the composition in the following ratio – 50% of additive to the epoxy binder, 50% of additive to the PEPA hardener;
- mechanical combination epoxy oligomer and nano-dispersed condensed carbon during – 1 ± 0.1 min;
- ultrasonic treatment (UST) – 1.5 ± 0.1 min;
- cooling the composition (273 K) – 60 ± 5 min;
- mechanical combination of PEPA and nano-dispersed condensed carbon during – 1 ± 0.1 min;
- ultrasonic treatment (UST) – 1.5 ± 0.1 min;
- combination of two compositions (ED-20 with nano-dispersed condensed carbon + PEPA with nano-dispersed condensed carbon) during the time – 5 ± 0.1 min.

Then the polymerization of polymers under the set conditions is carried out [23-25]: time of the formation polymers – 12.0 ± 0.1 h (temperature – 293 ± 2 K), heat treatment of polymers at the temperature – 393 ± 2 K (during the time – 2.0 ± 0.05 h), cooling to the temperature – 293 ± 2 K.

2.3. Research Methods

The advantage of the proposed technology over existing solutions is a simplified forming technology, which provides for a reduction in costs for the production of new materials; it allows forming materials in the conditions of a ship, making it possible to transport and store such materials on the ship on the one hand and to ensure high operational characteristics (compared to analogues) on the other hand.

The structural changes that occur when the developed polymer materials are heated were studied using methods of thermogravimetric (TGA) and differential thermal analysis (DTA) was used, and derivatograph “Thermoscan-2” was applied [19, 25, 31]. Polymeric materials were studied in a range of temperatures $\Delta T = 298-873$ K, using quartz crucibles for specimens with the volume of $V = 0.5$ cm³ [19]. The rate of increase in temperature was $\nu = 5$ K/min, moreover, the reference substance was Al₂O₃ ($m = 0.5$ g) [25]. The error of determining the temperature was $\Delta T = \pm 1$ K [31]. The accuracy of determining thermal effects was 3 J/g. The accuracy of determining in the weight was – $\Delta m = 0.02$ g [19].

The activation energy was determined by the Broido's method [25, 29]. The condition for using this method was the first order decomposition reaction, which applied to both thermosetting and thermoplastic polymers. The loss of mass of a substance is a process of the 1st order ($n = 1$), if the linear dependence of $\ln(100 / (100 - \Delta m))$ on the inverse temperature $103/T$, K⁻¹. To determine the activation energy, a line was constructed, line in which E must be expressed by the tangent of the angle of the logarithmic dependence Δm on the in-verse temperature T (Fig. 1). Energy activation of thermal destruction can be calculated by (1):

$$E_a = -R \cdot \text{tg}(\varphi) \quad (1)$$

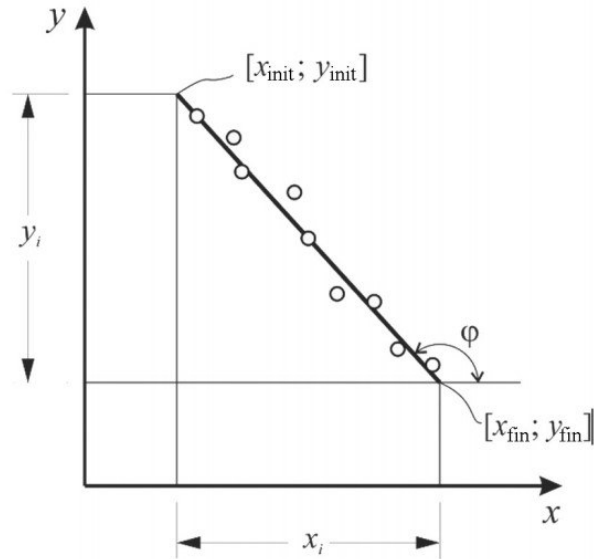


Figure 1. Graphical determination of activation energy.

To graphically determine the activation energy of thermal destruction, the graph should have a straight line, the tangent of the angle of inclination φ of which it is possible to calculate the activation energy E_a (Fig. 1) [25].

Then [29],

$$-\operatorname{tg}(\varphi) = y_i / x_i, \quad (2)$$

$$E = R \cdot y_i / x_i, \quad (3)$$

where $x_i = x_{\text{init}} - x_{\text{fin}}$ – the length of the line along the abscissa;

$y_i = y_{\text{init}} - y_{\text{fin}}$ – the length of the line along the ordinate;

$[x_{\text{init}}; y_{\text{init}}]$ and $[x_{\text{fin}}; y_{\text{fin}}]$ – coordinates of the beginning and end of the line, respectively.

With the use of modern research methods IR spectral analysis, the mechanisms of physical and chemical interaction of the binder with nano-additives and their change during operation will be established [25]. The IR-spectra were recorded on spectrophotometer "IRAffinity-1" (Japan) in the field of wave numbers $\nu = 400-4000 \text{ cm}^{-1}$ by a single-beam method in the reflected light. The wavelength scanning by wave numbers $\lambda^{-1} = \nu$ was performed on the diagram within 225 mm in the range of selected frequencies. Wave numbers, the intensity of passage, half-width and area of the absorption band were determined using a computer program called IRsolution. The error of determining the wave number was $\nu = \pm 0.01 \text{ cm}^{-1}$, and the error of determining the peak location was $\nu = \pm 0.125 \text{ cm}^{-1}$. The photometric accuracy was $\pm 0,2\%$ in case of a programmed control of a slit and the duration of integration $t = 10 \text{ s}$. The integration step was $\Delta\lambda = 4 \text{ cm}^{-1}$. The IR-spectral analysis of nanocomposites was performed with the optimal content of nanoparticles at different stages of thermal degradation. The material was crushed, dried at a temperature of $T = 373 \text{ K} \pm 2$ during $t = 20 \text{ min}$, stirred in an agate mortar with the KBr powder, and then specimens were formed on a hydraulic press with loading of $\sigma = 20 \text{ MPa}$ in the following proportion: study material – 1 mg, KBr – 300 mg [25].

3. Discussion

3.1. Thermogravimetric analysis (TGA) of composites filled with a nano-dispersed condensed carbon

The thermal stability of polymers is one of the important characteristics that allows such materials to be used in different temperature ranges [20-22]. At the same time, thermal analysis is a method for determining the thermophysical properties of polymers and studying their temperature transitions. Therefore, previously in the work, the heat resistance of reactive plastic polymer materials (temperature range – 303-873 K) [19, 25]. TGA analysis made it possible to establish the absence of mass loss for the developed nanocomposite materials in the temperature – 303-624 K (Fig. 2, Table 1).

Table 1. Structural changes of polymers under the influence of temperature

Content of a nano-dispersed condensed carbon, %	T_0 , K	T_5 , K	T_{10} , K	T_{20} , K	T_f , K	ε_m , %
0.025	618.0	619.8	633.3	646.6	714.0	63.3
0.050	624.9	628.5	634.6	648.1	718.7	60.3
0.075	556.3	616.5	629.2	641.7	714.0	69.3
0.100	610.0	620.3	630.9	642.8	712.4	70.0

Structural changes of the unfilled polymer matrix occurred at $T_0 = 587$ K [25]. Changing the content of nanofiller in the epoxy binder (0.025-0.100 pts.wt.) allowed shifting the initial temperature of mass loss by 37.0-47.9 K to the area of high temperatures.

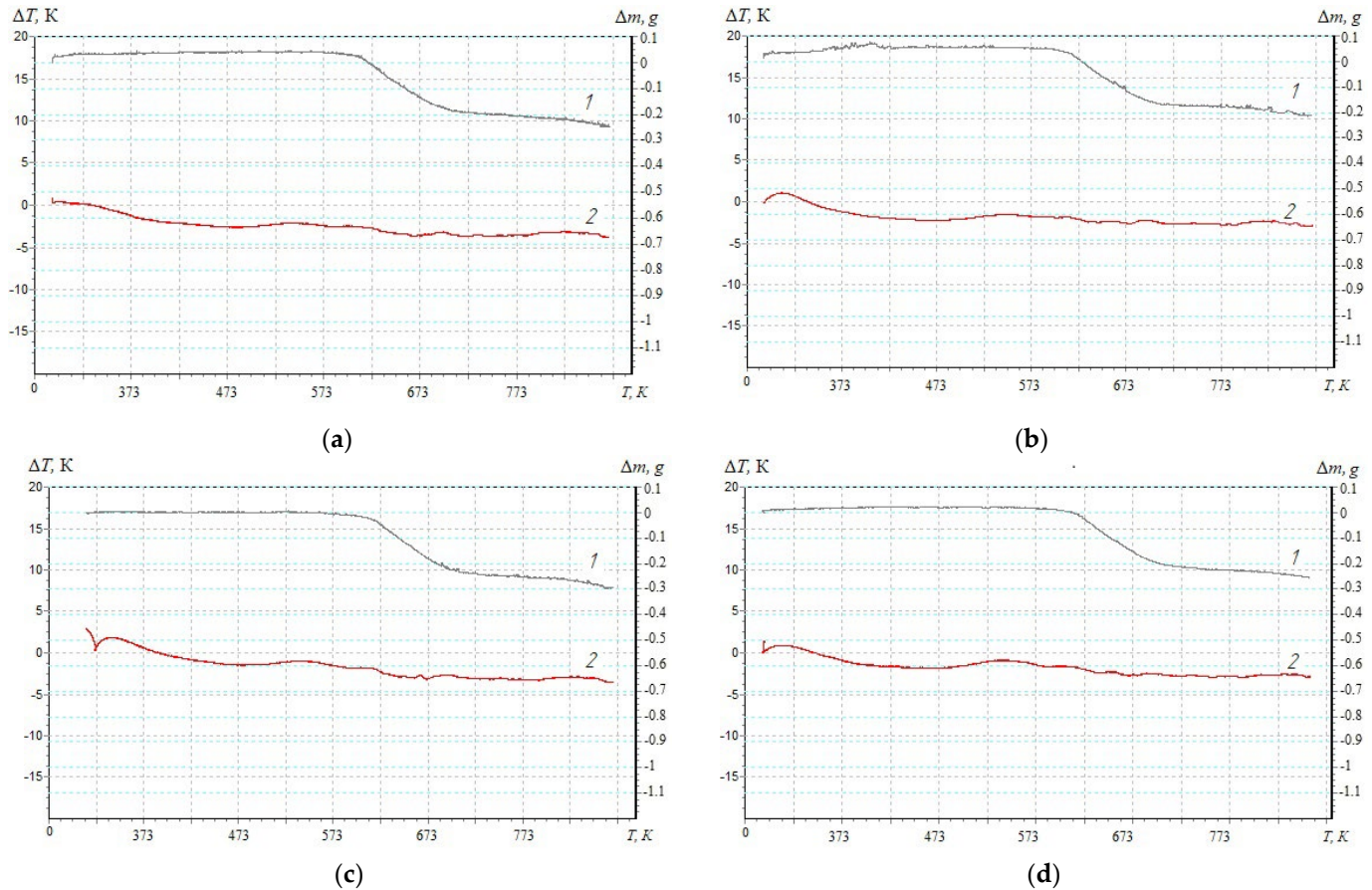


Figure 2. Thermal analysis of composites materials filled with a nano-dispersed condensed carbon: a) 0.025 %; b) 0.050 %; c) 0.075 %; d) 0.100 %; 1 – thermogravimetric (1) analysis; 2 – differential-thermal (2) analysis

Polymers filled with nano-dispersed condensed carbon (0.050 pts.wt.) were characterized by the highest temperature of the beginning of mass loss (among the investigated nanocomposites) (Table 1), which makes it possible to claim inhibition of thermo-oxidative destruction reactions by limiting the mobility of segments of the polymer network and the main chain. The end of the destruction process of the developed composites was observed in the temperature – 712-718 K. At the same time, the difference mass loss of the unfilled matrix (80.7%) [25] and filled composites (63-70%), indicating the presence of a nano-additive that undergoes thermal transformations under the influence of a higher temperature.

3.2. Calculation of the activation energy of thermal destruction of composite materials filled with a nano-dispersed condensed carbon

To assess the degree of crosslinking of composite materials filled with nano-dispersed condensed carbon, the activation energy of thermal destruction is calculated according to the Broido method [25, 29, 31]. TGA curves (Fig. 2, Curve 1) are used to mathematically calculate the activation energy, which are analyzed in the temperature range $\Delta T = 573-713$ K (Fig. 3), which corresponds to the loss of mass of polymers $T_{5-90\%}$, K. Previously, the mass loss of materials with an interval of $\Delta T = 10$ K (Fig. 3) for a composite filled with NCC (0.050 pts.wt.) is determined. Similarly, research is conducted for composites with different contents of nanofiller (Tables 2-4).

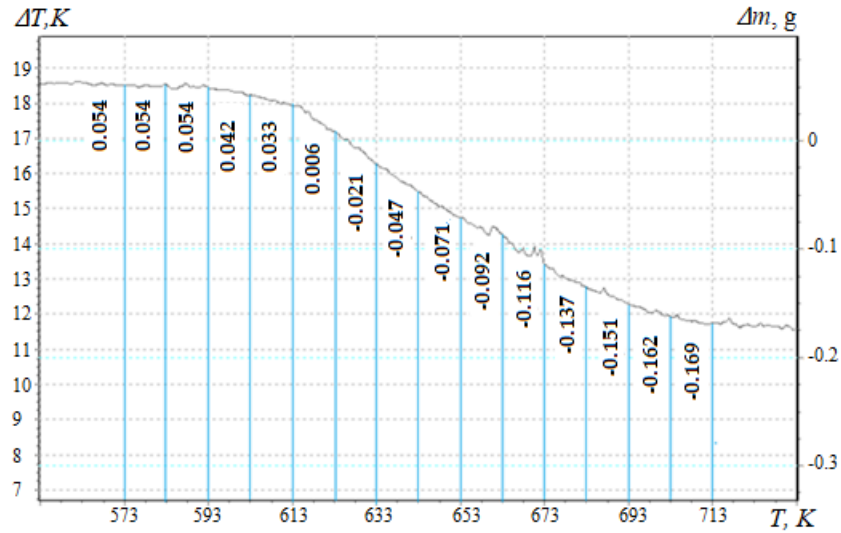


Figure 3. Mass loss of a composite material filled with nano-dispersed condensed carbon (0.050 pts.wt.)

The mass value of the studied composite material is calculated as a percentage using E_q (4).

$$(100 - \Delta m)\% = \left(100 - \left(\frac{m_{in} + \Delta m}{\Delta m} \cdot 100 \right) \right)\%, \quad (4)$$

where m_{in} – sample mass at the temperature ($T_1 = 573 \text{ K} = \text{const}$);

Δm – mass of the polymer as the temperature increases.

The mass of the composite material at the initial temperature is taken as 100%. Table 2 shows the results of processing the TGA curves and the parameters necessary to calculate the energy activation of composites filled with NCC.

Table 2. Change of the polymers mass according to the results of TGA analysis

T, K	Sample mass (100-Δm), %			
	Content of a nano-dispersed condensed carbon, q, wt. %			
	0.025	0.050	0.075	0.100
573	-12.33	-18.62	2.07	-6.21
583	-12.33	-17.93	2.41	-4.83
593	-10.67	-17.24	3.10	-3.10
603	-9.00	-14.48	6.21	-1.72
613	-5.33	-11.38	10.00	1.38
623	2.67	-2.07	16.21	8.62
633	14.00	7.24	25.52	18.62
643	22.67	16.21	35.17	27.59
653	29.67	24.48	44.14	35.86
663	36.67	31.72	54.14	45.86
673	45.33	40.00	62.76	53.10
683	52.33	47.24	70.00	60.00
693	56.67	52.07	75.52	65.86
703	61.33	55.86	82.76	70.00
713	63.00	58.28	84.83	72.07

The activation energy was determined by the Broido's method, according to works [25, 29, 31]:

$$\ln\left(\ln\frac{100}{100-\Delta m}\right) = -\frac{E}{R} \cdot \frac{1}{T} + const \quad (5)$$

The results of calculations of the value of the double logarithm of the change in the mass of the samples are given in Table. 3.

Knowing the mass loss (Δm) of composites filled with nano-dispersed condensed carbon at temperature T , a straight line is graphically constructed, in which E is determined by the tangent of the slope angle of the logarithmic dependence of Δm on the inverse temperature T .

Table 3. Calculated logarithmic dependence of mass on the reciprocal temperature

T, K	$\ln\{\ln[100/(100-\Delta m)]\}$			
	Content of a nano-dispersed condensed carbon, $q, wt.\%$			
	0.025	0.050	0.075	0.100
573	–	–	-3.868	–
583	–	–	-3.712	–
593	–	–	-3.457	–
603	–	–	-2.748	–
613	–	–	-2.250	-4.277
623	-3.611	–	-1.733	-2.406
633	-1.892	-2.588	-1.222	-1.580
643	-1.359	-1.733	-0.836	-1.131
653	-1.044	-1.270	-0.541	-0.812
663	-0.784	-0.963	-0.249	-0.488
673	-0.504	-0.672	-0.012	-0.278
683	-0.300	-0.447	0.186	-0.087
693	-0.179	-0.307	0.342	0.072
703	-0.051	-0.201	0.564	0.186
713	-0.006	-0.135	0.634	0.243

Destruction activation energy is found by Eq (1). Fig. 4 shows graphical dependences of the rate of destruction on the inverse temperature, and Table 4 shows the analytical results of the graphical determination of the activation energy of the developed CM

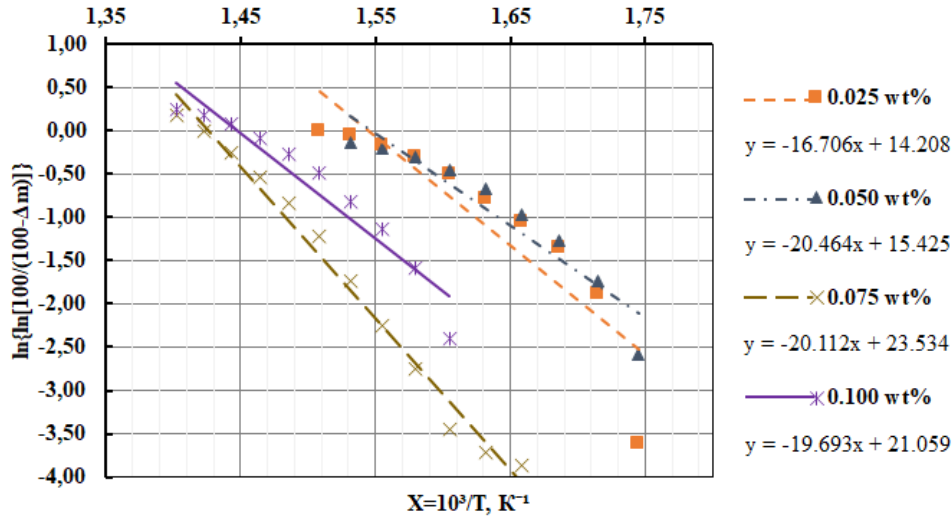


Figure 4. Graphical dependence of the epoxy composites materials filled with a nano-dispersed condensed carbon destruction rate on the inverse temperature

Table 4. Activation energy of polymers materials filled with a nano-dispersed condensed carbon

Content of a nanodispersed condensed carbon, q , wt. %	X_{HD}	X_k	X_i	Y_H	Y_k	Y_i	$tq(\varphi)$	Energy activation E_a , kJ/mol
0.025	1.605	1.403	0.202	-9.230	-12.605	3.375	16.706	138.8
0.050	1.580	1.403	0.177	-13.286	-16.908	3.622	20.464	170.1
0.075	1.745	1.403	0.342	-4.863	-11.741	6.878	20.112	167.2
0.100	1.631	1.403	0.228	-6.5703	-11.060	4.490	19.693	163.7

Note: X_{HD} – coordinates of the length of the line along the abscissa axis (start); X_k – coordinates of the length of the line along the abscissa axis (end); X_i – the length of the line along the abscissa axis; Y_H – coordinates of the length of the line along the ordinate axis (start); Y_k – coordinates of the length of the line along the abscissa axis (end); Y_i – the length of the line along the abscissa axis; $tq(\varphi)$ – the tangent of the slope angle φ of the logarithmic dependence

Based on the calculations, it was found that for the thermal destruction of the composite filled with NCC (0.050 pts.wt.) the highest thermal energy ($E_a = 170.1$ kJ/mol) was required (Table 4).

3.3. Differential thermal analysis (DTA) of composites filled with a nano-dispersed condensed carbon

To register thermal effects and determine the ignition temperature of the developed nanocomposites, differential thermal (DTA) analysis is used (Fig. 5). It was found that the maximum value of the initial temperature of the exoeffect – $T_{init} = 486.8$ K was typical for composites filled with NCC particles with a content of $q = 0.050$ pts.wt. (Table 5).

The initial temperature of the exoeffect corresponds to the beginning of thermal oxidation of the composite, since no mass loss is observed on the TGA curves (Fig. 2). At the same time, there is a possibility of a carbonized layer on the surface of the polymer (as a result of oxidation when the polymer is heated), which acts as a heat-insulating layer that limits the access of the oxidant, thereby suppressing the destruction of the polymer.

Table 5. Structural change of polymers according to the results of DTA analysis

Content of a nano-dispersed condensed carbon, q , wt. %	Temperature intervals of exoeffects				Maximal temperature exoeffects, T_{max} , K	
	T_{init} , K	T_f' , K	ΔT_1 , K	ΔT_2 , K	T_{max} , K	
					Peak1 / T_{max1}	Peak 2 / T_{max2}
0.025	485.5	666.3	184.8	1.50	545.5	683
0.050	486.8	676.3	193.5	0.73	553.3	692
0.075	471.7	670.6	198.9	2.18	540.1	674
0.100	460.0	670.5	210.5	2.39	542.2	680

Note: T_{max1} – exoeffect maximum value composites; T_{max2} – the oxidation temperature of the nanoadditive

At the same time, analyzing the DTA and TGA curves, a loss of polymer mass was observed after the maximum value of the exoeffect (T_{max1}), which indicated the release of gaseous products due to the increase in temperature and the loss of the heat-insulating carbonized layer.

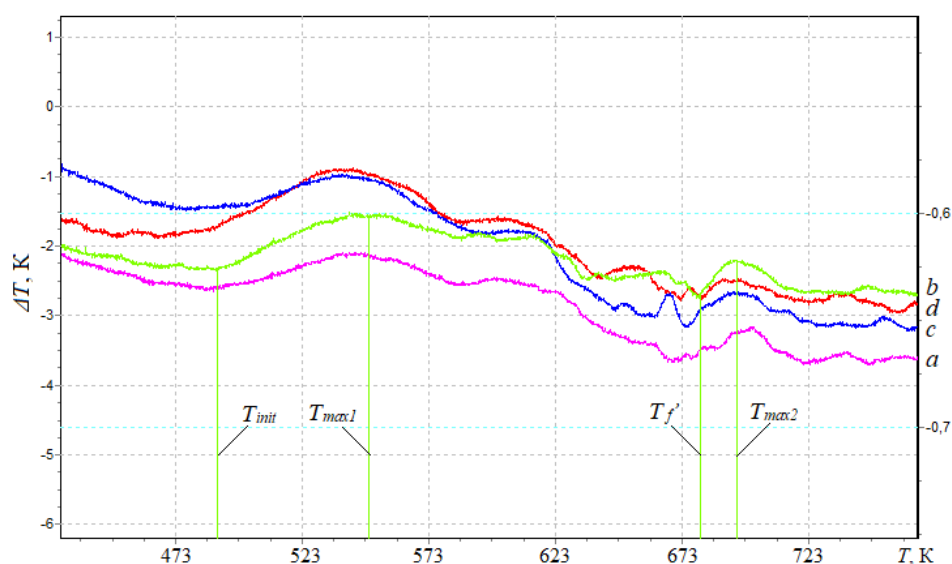


Figure 5. Determination of thermal effects by the method of differential thermal analysis of composites filled with nano-dispersed condensed carbon: a) 0.025 pts.wt.; b) 0.050 pts.wt.; c) 0.075 pts.wt.; d) 0.100 pts.wt.

Based on the analysis of DTA curves, two peaks with characteristic maxima for filled composites are established (Table 5, Fig. 5). It is believed that T_{max1} corresponds to the temperature at which increased mobility and deformation of bonds occurs due to the structural changes of the nanocomposite, while the oxidation process was replaced by dissociation processes – chemical and physical decomposition of the oxidized component. While T_{max2} corresponds to the oxidation temperature of the nano-additive, which in order of magnitude coincides with the characteristics of the filler (the oxidation temperature of the nano-filler is 583-623 K). Thus, the thermal effects of T_{max1} will be greater than T_{max2} in absolute value and time parameters of the course of the thermal reaction. At the same time, for the quantitative analysis and practical application of the developed polymer materials, the most informative is the initial temperature of the exoeffect (T_{init}), the maximum value of the exoeffect (T_{max1}), at which the structural changes of the composites. At the same time, the final temperature of the exoeffect (T_f') is also important, since in this temperature range the activation energy is determined by a mathematical method, which makes it possible to estimate the degree of crosslinking of the polymer. Analyzing the final temperature of the exoeffect, an increase in the activation energy is established from $E_a = 138.8$ kJ/mol ($q = 0.025$ pts.wt.) to $E_a = 170.1$ kJ/mol ($q = 0.050$ pts.wt.), which indicates the stability of physical-chemical bonds to destruction under the influence of temperature due to the arrangement of the structure of the polymer. Then, as the introduction of nanofiller into the polymer at a content of $q = 0.075$ -0.100 pts.wt. ensures a decrease in the value of the activation energy, which can be caused by agglomeration of the additive in the volume of the polymer.

3.4. IR spectral analysis of composites filled with a nano-dispersed condensed carbon.

In order to confirm the above provisions and specify the permissible temperature range at which it is possible to use the developed nanocomposites, an IR spectral analysis was additionally performed (Fig. 6). Registration and analysis of IR spectra were carried out in stages, in order of increasing temperature (Fig. 5). First, the IR spectrum of the composite with the optimal content of

nanodispersed condensed carbon, which is not exposed to the influence of temperature (Fig. 6, spectrum 1), was obtained. That is, it is the IR spectrum of the control sample which others are compared that is exposed to the influence of temperature. Then, the IR spectrum of the composite filled with NCC is recorded with a content of $q = 0.050$ pts.wt. (Fig. 6, spectrum 2) at the initial temperature of the exoeffect $T_{init} = 486$ K (Fig. 5).

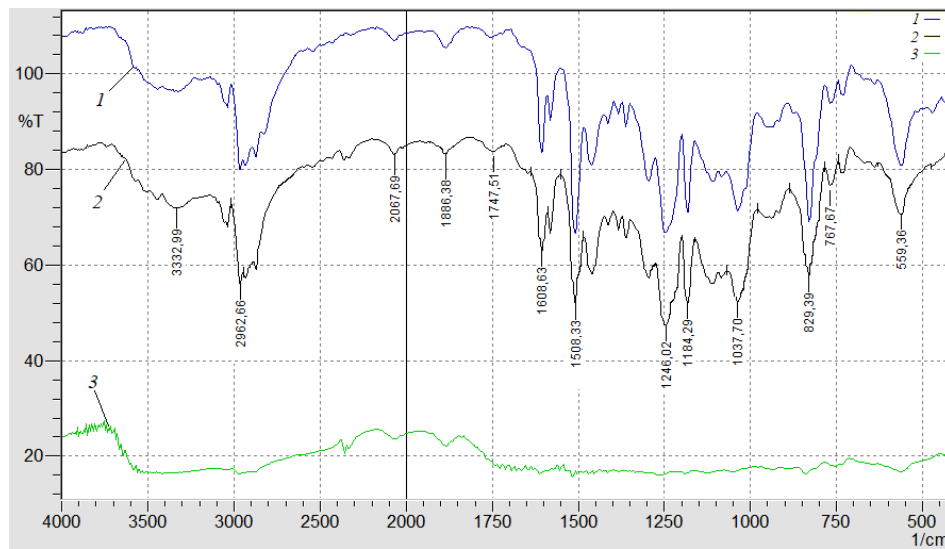


Figure 6. IR spectral analysis of the polymers (0.050 pts.wt.): 1 – control sample spectrum; 2 – NCC spectrum at the initial temperature of the exoeffect; 3 – NCC spectrum at the maximum value of the exoeffect

Decrease in the relative value of the peak area from $S = 18.9\%$ to $S = 16.1\%$ at the wave number $\nu = 559$ cm^{-1} was observed (Fig. 6, Spectrum 2). This indicates the deformation fluctuations of the aliphatic chain -C-H- with increasing temperature. In addition, a decrease in the relative value of the peak area in the range of wave numbers $\nu = 829\text{-}1246$ cm^{-1} was also observed, which indicates the mobility and deformation of the macromolecule segments of the ED-20 epoxy oligomer and C-C bonds of the aromatic ring. A decrease in the relative value of the peak area from $S = 14.4\%$ to $S = 12.3\%$ at $\nu = 1508$ cm^{-1} indicates increased mobility and deformation of the amine groups of the polymer. The analysis of the IR spectrum in the range of wave numbers $\nu = 1608\text{-}3332$ cm^{-1} allows stating that there are no significant structural changes in the polymer.

In the future, the IR spectrum of the composite filled with NCC is recorded (Fig. 6, Spectrum 3) at the temperature $T_{max1} = 553.3$ K (Fig. 5). A further decrease in the relative value of the peak area from $S = 16.1\%$ (Fig. 6, Spectrum 3) to $S = 2.1\%$ (Fig. 6, Spectrum 3) at the wave number $\nu = 559$ cm^{-1} was observed, which indicates the destruction of the aliphatic chain -C-H- . In the $\nu = 767\text{-}1747$ cm^{-1} , the absence of peaks was observed, which indicates the destruction of a significant number of epoxy amine, C-C-, -C-H- groups. At wave numbers $\nu = 1886\text{-}3332$ cm^{-1} , no destruction of physical and chemical bonds was detected, only a decrease in the relative size of the peak area was observed. This indicates the resistance of C=O, C-H, O-H groups of the polymer to the influence of the above-mentioned temperature. Therefore, the decrease in the relative size of the peak area and their absence at the wave numbers $\nu = 767\text{-}1747$ cm^{-1} (at T_{max1}) confirms the assumption made earlier about the mobility and deformation of the bonds due to dissociation of the nanocomposite.

It should be noted that (T_{max2}) was not given in the work, since the use of the developed materials in these temperature ranges was not relevant due to the destruction of a significant number of chemical bonds.

4. Conclusions

The results of studies of the effect of nano-dispersed condensed carbon on the course of thermal transformations of polymer composite materials allow drawing the following conclusions. The change in the mass of polymer materials in the temperature range $\Delta T = 303\text{-}873$ K is determined by the method of thermogravimetric analysis, which made it possible to assess the stability of their physical and chemical bonds under the influence of a thermal field. It is proven that composites with a nanofiller content of $q = 0.050$ pts.wt. are characterized by the lowest initial mass loss temperature $T_0 = 624$ K. The stability of physico-chemical bonds to the influence of temperature of the developed nanocomposites is determined by Broido's method. It was found that nanocomposites containing $q = 0.050$ pts.wt. were characterized by the highest heat resistance of nanodispersed condensed carbon, since the maximum value of the activation energy (among the studied nanocomposites) was $E_a = 170.1$ kJ/mol. On the basis of the differential thermal and IR spectral analysis of the developed nanocomposites, it was proven that no absorption bands were found in the temperature range $\Delta T = 303\text{-}486$ K. That is, the absence of structural transformations (destruction of chemical bonds) made it possible to use the developed materials up to the maximum temperature $T = 486$ K. The behavior of the developed materials at temperatures $T_{max1} = 553$ K (ignition temperature) and $T < 553$ K deserves special attention. It was not possible to use such materials, since the destruction of a large number of bonds of the nanocomposite was observed.

We have developed a new, simplified technology for the formation of epoxy materials (Materials and methods). The advantage of the proposed technology over existing solutions is a simplified forming technology, which provides for a reduction in costs for the

production of new materials; it allows forming materials in the conditions of the ship, making it possible to transport and store such materials on the ship on the one hand and to ensure high operational characteristics (compared to analogues) on the other hand. A new approach to determining the maximum temperature at which it is possible to use new materials without changing their properties is presented. It consists of a combination of modern research methods (DTA, IR spectral analysis) and mathematical methods of researching exothermic reactions that occur when polymer materials are heated.

Author Contributions: Methodology, O.S.; Resources, P.V., L.S.; Writing—original draft, A.B.; Visualization, B.K. All authors have read and agreed to the published version of the manuscript.

Funding: This research received no external funding.

Conflicts of Interest: The authors declare no conflict of interest.

References

1. Dobrotvor, I.G., Stukhlyak, P.D., Mykytyshyn, A.G., Stukhlyak, D.P. Influence of Thickness and Dispersed Impurities on Residual Stresses in Epoxy Composite Coatings. *Strength of Materials*. **2021**, 53(2), 283–290/
2. Demchenko, V., Kobylinskyi, S., Iurzhenko, M., Riabov, S., Vashchuk, A., Rybalchenko, N., Zahorodnia, S., Naumenko, K., Demchenko, O., Adamus, G., Kowalczyk, M. Nanocomposites based on polylactide and silver nanoparticles and their antimicrobial and antiviral applications. *Reactive and Functional Polymers*. **2022**, 170, 105096.
3. Saponov, O., Maruschak, P., Sotsenko, V., Buketova, N., de Deus, A.B.D.G., Saponova, A., and Prentkovskis, O., Development and Use of New Polymer Adhesives for the Restoration of Marine Equipment Units. *J. Mar. Sci. Eng.* **2020**, 8(7), 527.
4. Stukhlyak, P.D., Holotenko, O.S., Dobrotvor, I.H., and Mytnyk, M.M., Investigation of the Adhesive Strength and Residual Stresses in Epoxy Composites Modified by Microwave Electromagnetic Treatment. *Mater. Sci.* **2015**, 51(2), 208–12.
5. Buketov, A.V., Saponov, O.O., Brailo, M.V. Investigation of the Physico-Mechanical and Thermophysical Properties of Epoxy Composites with a Two-Component Bidisperse Filler. *Strength of Materials*. **2014**, 46(5), 717–723.
6. Demchenko, V.L., Kobylinskyi, S.M., Riabov, S.V., Shtompel V.I., Iurzhenko, M.V., Rybalchenko, N.P., Novel approach to the formation of silver-containing nanocomposites by thermochemical reduction of Ag⁺ ions in interpolyelectrolyte-metal complexes. *Applied Nanoscience*. **2020**, 10(12), 5409–5419.
7. Chykhira, I.V., Stukhlyak, P.D., Mytnyk, M.M., Kartashov, V.V. Investigation of epoxycomposites linking kinetics during ultrasonic treatment. *Functional Materials*. **2021**, 28(1), 84–89/
8. Kashytskiy, V., Savchuk, P., Malets, V., Herasymyuk, Y., and Shcheglov, S., Examining the Effect of Physical Fields on the Adhesive Strength of Protective Epoxy Composite Coatings. *East.-Eur. J. Enterprise Technol.* **2017**, 3, 16–22.
9. Panda, A., Dyadyura, K., Valiček, J., Harničárová, M., Kušnerová, M., Ivakhniuk, T., Hrebenyk, L., Saponov, O., Sotsenko, V., Vorobiov, P., Levytskyi, V., Buketov, A., Pandová, I., Ecotoxicity Study of New Composite Materials Based on Epoxy Matrix DER-331 Filled with Biocides Used for Industrial Applications. *Polymers*. **2022**, 14, (16):3275.
10. Buketov, A., Saponov, O., Brailo, M., Stukhlyak, D., Yakushchenko, S., Buketova, N., Saponova, A., Sotsenko V. The Use of Complex Additives for the Formation of Corrosion- and Wear-Resistant Epoxy Composites. *Advances in Materials Science and Engineering*. **2019**, Article ID 8183761, 5.
11. Totosko, O., Stukhlyak, P., Mykola, M., Dolgov, N., Zolotiy, R., Stukhlyak, D., Investigation of Corrosion Resistance of Two-Layer Protective Coatings. *Challenges to National Defence in Contemporary Geopolitical Situation*. **2022**, 1, 50–54.
12. Sironmani, Palraj, Muthiah, Selvaraj, Kuppaiyanpoosari, Maruthan, Gopalakrishnan, Rajagopal, Corrosion and wear resistance behavior of nano-silica epoxy composite coatings. *Progress in Organic Coatings*. **2015**, 81, 132–139.
13. Kashiwagi, T., Du, F., Douglas, J. et al, Nanoparticle networks reduce the flammability of polymer nanocomposites. *Nature Mater.* **2005**, 4, 928–933.
14. Xueming Sun, Zhiwei Li, Oisik Das, Mikael S. Hedenqvist., Superior flame retardancy and smoke suppression of epoxy resins with zinc ferrite@polyphosphazene nanocomposites. *Composites Part A: Applied Science and Manufacturing*. **2023**, 167, 107417.
15. Hong, Jing, Wu, Tong, Wu, Haiyang, Zeng, Birong, Zeng, Shanni, Chen, Ting, Wang, Xiu, Lu, Zhenwu, Yuan, Conghui, Balaji, Krishnasamy, Petri, Denise F.S., Dai, Lizong., Nanohybrid silver nanoparticles@halloysite nanotubes coated with polyphosphazene for effectively enhancing the fire safety of epoxy resin. *Chemical Engineering Journal*. **2020**, 127087.
16. B. Yu, Y. Shi, B. Yuan, S. Qiu, W. Xing, W. Hu, L. Song, S. Lo, and Y. Hu. Enhanced thermal and flame retardant properties of flame-retardant-wrapped graphene/epoxy resin nanocomposites. *J. Mater. Chem. A* (5). **2015**, 8034–8044.
17. Qian, X., Song, L., Yu, B., Wang, B., Yuan, B., Shi, Y., Hu, Y., Yuen, R.K.K., Novel organic–inorganic flame retardants containing exfoliated graphene: preparation and their performance on the flame retardancy of epoxy resins. *J. Mater. Chem. A* 1. **2013**, 1(23), 6822.
18. Buketov, A.V., Dolgov, N.A., Saponov, A.A., Nigalati V.D. Adhesive pull and shear strength of epoxy nanocomposite coatings filled with ultradispersed diamond. *Strength of Materials*. **2018**, 50(3), 425–431.
19. Kholodovych, V., Welsh, W.J., Thermal-oxidative stability and degradation of polymers, In: Mark JE, editor. Physical properties of polymers handbook. *New York: Springer New York*. **2007**, 54, 927–938.
20. Davies, M., Wang, Y., Wong, P., Polymer composites in fire. *Composites Part A: Applied Science and Manufacturing*. **2006**, 37(8), 1131–1141.
21. Morgan, A.B., and Gilman, J.W., An overview of flame retardancy of polymeric materials: application, technology, and future directions. *Fire and Materials*. **2012**, 37, 259–279.

22. Mohamed Bakar, Wojciech Kucharczyk, Sylwester Stawarz and Wojciech Żurowski. Effect of nanopowders (TiO₂ and MMT) and aramid honeycomb core on ablative, thermal and dynamic mechanical properties of epoxy composites. *Journal: Composite Structures*. **2021**, 259, 113450.
23. Buketov, A.V., Brailo, M.V., Yakushchenko, S.V., Sapronov, O.O., Smetankin, S.O. The formulation of epoxy-polyester matrix with improved physical and mechanical properties for restoration of means of sea and river transport. *Journal of Marine Engineering & Technology*. **2020**, 19(3), 109–114.
24. Sapronov, O., Maruschak, P., Buketova, N., Leschenko, O., and Panin, S., Investigation of PM-75 Carbon Black Addition on the Properties of Protective Polymer Coatings. *AIP Conf. Proc.* **2016**, 020194.
25. Sapronov, O.O., Buketov, A.V., Zinchenko, D.O., Yatsyuk V.M., Features of structural processes in epoxy composites filled with silver carbonate on increase in temperature. *Composites: Mechanics, Computations, Applications. An International Journal*. **2017**, 8, (1), 47–65.
26. Régnier, N., Fontaine, S., Determination of the thermal degradation kinetic parameters of carbon fibre reinforced epoxy using TG. *J. Therm. Anal. Calorim.* **2021**, 64(2), 789-799.
27. Brnardic, I., Macan, J., Ivankovic, H., Ivankovic, M., Thermal degradation kinetics of epoxy/organically modified montmorillonite nanocomposites. *J. Appl. Polym. Sci.* **2008**, 107(3), 1932–1938.
28. Jojibabu, P., Ram, G. D. J., Deshpande, A. P., & Bakshi, S. R., Effect of carbon nano-filler addition on the degradation of epoxy adhesive joints subjected to hygrothermal aging. *Polymer Degradation and Stability*. **2017**, 140, 84–94.
29. Burya, A. I., Naberezhnaya, O. A., & Arlamova, N. T., Investigation of the thermal destruction process of aromatic polyamides and organic plastics based on them. *Journal of Characterization and Development of Novel Materials*. **2015**, 7(2), 171.
30. Buketov, A., Sapronov, O., Klevtsov, K., Kim, B. Functional Polymer Nanocomposites with Increased Anticorrosion Properties and Wear Resistance for Water Transport. *Polymers*. **2023**, 15: 3449.
31. Yakushchenko, S.V., Brailo, M.V., Buketov, A.V., Sapronov, O.O., Popovych, V., Dulebova, L, Investigation of the properties and structure of epoxy–polyester composites with two-component bidispersed filler. *Composites: Mechanics, Computations, Applications, An International Journal*. **2022**, 13(1), 81–95.
32. Roy, S., Mitra, K., Desai Ch. et al., Detonation nanodiamonds and carbon nanotubes as reinforcements in epoxycomposites – A Comparative study. *Journal of Nanotechnology in Engineering and Medicine*. **2013**, 4 (1), 1–7.
33. Li, Y., Huang, X., Zeng, L., Li, R., Tian, H., Fu, X., Wang Yu., Zhong, W.-H., A review of the electrical and mechanical properties of carbon nanofiller-reinforced polymer composites. *Journal of Materials Science*. **2019**, 1–41.